Published February 9, 2009

Phospholipase C–mediated hydrolysis of PIP2 releases ERM proteins from lymphocyte membrane

Jian-Jiang Hao,[1] Yin Liu,[1] Michael Kruhlak,[1] Karen E. Debell,[2] Barbara L. Rellahan,[2] and Stephen Shaw[1]

[1]Experimental Immunology Branch, National Cancer Institute, National Institutes of Health, Bethesda, MD 20892
[2]Center for Drug Evaluation and Research, Food and Drug Administration, Bethesda, MD 20892

Mechanisms controlling the disassembly of ezrin/radixin/moesin (ERM) proteins, which link the cytoskeleton to the plasma membrane, are incompletely understood. In lymphocytes, chemokine (e.g., SDF-1) stimulation inactivates ERM proteins, causing their release from the plasma membrane and dephosphorylation. SDF-1–mediated inactivation of ERM proteins is blocked by phospholipase C (PLC) inhibitors. Conversely, reduction of phosphatidylinositol 4,5-bisphosphate (PIP2) levels by activation of PLC, expression of active PLC mutants, or acute targeting of phosphoinositide 5-phosphatase to the plasma membrane promotes release and dephosphorylation of moesin and ezrin. Although expression of phosphomimetic moesin (T558D) or ezrin (T567D) mutants enhances membrane association, activation of PLC still relocalizes them to the cytosol. Similarly, in vitro binding of ERM proteins to the cytoplasmic tail of CD44 is also dependent on PIP2. These results demonstrate a new role of PLCs in rapid cytoskeletal remodeling and an additional key role of PIP2 in ERM protein biology, namely hydrolysis-mediated ERM inactivation.

Introduction

Ezrin/radixin/moesin (ERM) proteins link the cortical cytoskeleton to the plasma membrane. In their active conformation, the N-terminal FERM (protein 4.1 ERM) domain binds to the cytoplasmic tails of transmembrane proteins, and the C-terminal ERM association domain (C-ERMAD) region binds to actin filaments (Bretscher et al., 2002; Fievet et al., 2007; Hughes and Fehon, 2007; Niggli and Rossy, 2008). However, ERMs also exist in a dormant or autoinhibited conformation in which the binding sites on the FERM domain are masked by the remainder of the molecule, including an ~200-residue linker and the C-ERMAD (Pearson et al., 2000; Li et al., 2007). Transition of ERM proteins to an active conformation (i.e., release of autoinhibition) occurs by two distinct mechanisms: (1) binding of the FERM domain to membrane rich in phosphatidylinositol 4,5-bisphosphate (PIP2) and (2) phosphorylation of the C-ERMAD. After a decade of elegant in vitro and in vivo studies, a dominant current view is that activation occurs in a two-step fashion (Bretscher et al., 2002; Fievet et al., 2007; Hughes and Fehon, 2007; Niggli and Rossy, 2008). First, PIP2 binding induces a conformational change and partial activation (Barret et al., 2000; Yonemura et al., 2002). Second, because that conformational change has made the phosphorylation site accessible, C-terminal phosphorylation can occur (Fievet et al., 2004). When phosphorylated, ERM proteins are active (Matsui et al., 1998; Huang et al., 1999; Nakamura et al., 1999). According to a recent study (Fievet et al., 2004), phosphorylated ERM (pERM) proteins are active without PIP2.

Although activation is the focus of studies of ERM protein regulation in most cells, ERM protein inactivation is also biologically important, particularly in cytoskeletal reorganization (Brown et al., 2001; Zeidan et al., 2008). Acute ERM protein inactivation plays a critical physiological role in lymphocytes. Lymphocyte recirculation from blood into tissue then back into blood is crucial for efficient immune responses (Laudanna and Alon, 2006; Rose et al., 2007). While in blood, the cytoskeleton of the lymphocyte assures that it is spherical and relatively rigid, allowing it to survive the hemodynamic rigors of circulation. Regulated binding to vascular endothelium and migration into tissue are triggered by molecules termed chemokines on the endothelial surface that activate G protein–coupled receptors (GPCRs) on the lymphocyte. One very rapid consequence is global reorganization of cytoskeleton into a configuration appropriate

Correspondence to Stephen Shaw: shaws@mail.nih.gov

Abbreviations used in this paper: 5-ptase, phosphoinositide 5-phosphatase; C-ERMAD, C-terminal ERM association domain; ERM, ezrin/radixin/moesin; GPCR, G protein–coupled receptor; mRFP, monomeric RFP; PBT, peripheral blood T cell; pERM, phosphorylated ERM; PH, pleckstrin homology; WB, Western blot; wt, wild type.

Supplemental Material can be found at:
http://jcb.rupress.org/content/suppl/2009/02/09/jcb.200807047.DC1.html

The Rockefeller University Press $30.00
J. Cell Biol. Vol. 184 No. 3 451–462
www.jcb.org/cgi/doi/10.1083/jcb.200807047

Published February 9, 2009

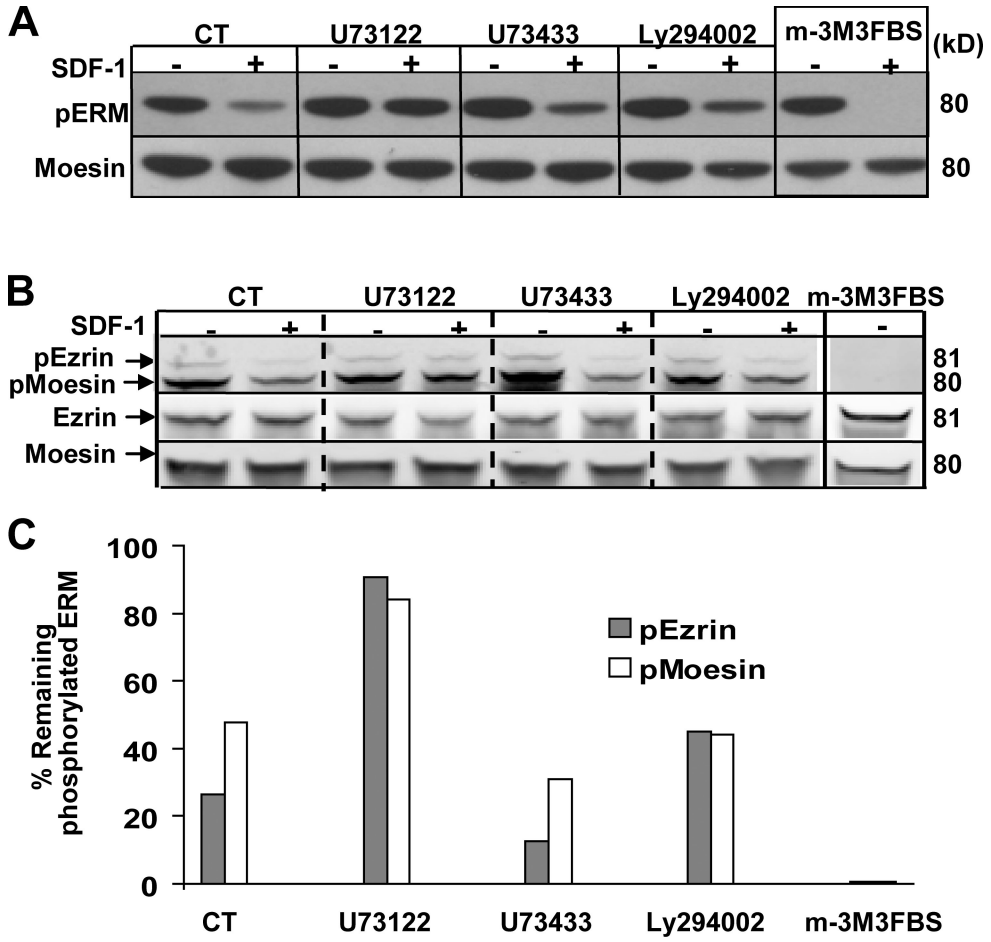

Figure 1. **SDF-1–induced ERM protein dephosphorylation depends on PLC signaling.** (A) Detection of ERM protein phosphorylation by WB in SDF-1–stimulated PBT. Freshly isolated PBTs from a healthy donor were preincubated with PLC inhibitor U73122, its nonfunctional analogue U73433, or PI3-K inhibitor Ly294002 for 10 min and stimulated with/without SDF-1 or PLC activator m-3M3FBS for 45 s. Note that phosphorylated moesin and ezrin are both present in PBT but run as a single band under these conditions. (B) Detection of both moesin and ezrin protein dephosphorylation by WB in SDF-1–stimulated PBT. The samples were prepared as in A but were resolved by running on SDS 4–20% Tris-glycine gels to separate moesin from ezrin. The top panel shows a blot for pERM; the top band is ezrin, and the bottom band is moesin. The middle and bottom panels show WB with antiezrin rabbit polyclonal antibody and antiezrin mouse mAb. (C) Quantitative analysis of data from B using Odyssey software (version 3.0; LI-COR Biosciences). CT, control.

for a flexible migration-capable cell (Brown et al., 2001). Because ERMs provide a conformationally regulated connection from the cortical actin cytoskeleton to the plasma membrane (Bretscher et al., 2002; Fievet et al., 2007; Hughes and Fehon, 2007; Niggli and Rossy, 2008), rapid conversion of ERMs from their active to inactive conformations plays a key role in this process (Brown et al., 2003; Ivetic and Ridley, 2004).

Proteins of the PLC family are critical mediators of signal transduction, especially for GPCRs such as chemokine receptors (Rhee, 2001). Proteins of this family are most widely known for their generation of two key mediators: a membrane-bound mediator, DAG, and a soluble mediator of Ca^{2+} release, IP3, which play multiple functions in diversified pathways. Less frequently discussed is the functional impact of local reduction of PIP2 in the plasma membrane that results from PLC-mediated hydrolysis of PIP2. Such changes in PIP2 have the potential to influence many molecules/processes such as ion channels and cytoskeleton (Janmey and Lindberg, 2004; McLaughlin and Murray, 2005).

We investigated the potential involvement of PIP2 and PLC in chemokine-induced ERM protein inactivation in lymphocytes based on (a) the importance of PIP2 in the aforementioned ERM activation and (b) the role of PLC in GPCR signaling, generally and specifically in chemokine-induced T lymphocyte migration (Bacon et al., 1995; Smit et al., 2003; Soriano et al., 2003; Cronshaw et al., 2006; Bach et al., 2007). We find that chemokine-induced inactivation of lymphocyte ERM proteins (ezrin and moesin) is mediated by the reduction of PIP2 that results from PLC hydrolysis. Moreover, our experiments reveal a key additional element not reflected in the Fievet model of sequential activation: even when ERM proteins are phosphorylated, their function largely depends on membrane PIP2.

Results

Activation of PLC is essential for SDF-1–induced ERM protein release from cortical membrane and dephosphorylation

We hypothesized that ERM protein inactivation might be one of the components of the migratory response that is dependent on PLC activation. The affect of PLC inhibitors on ERM

Published February 9, 2009

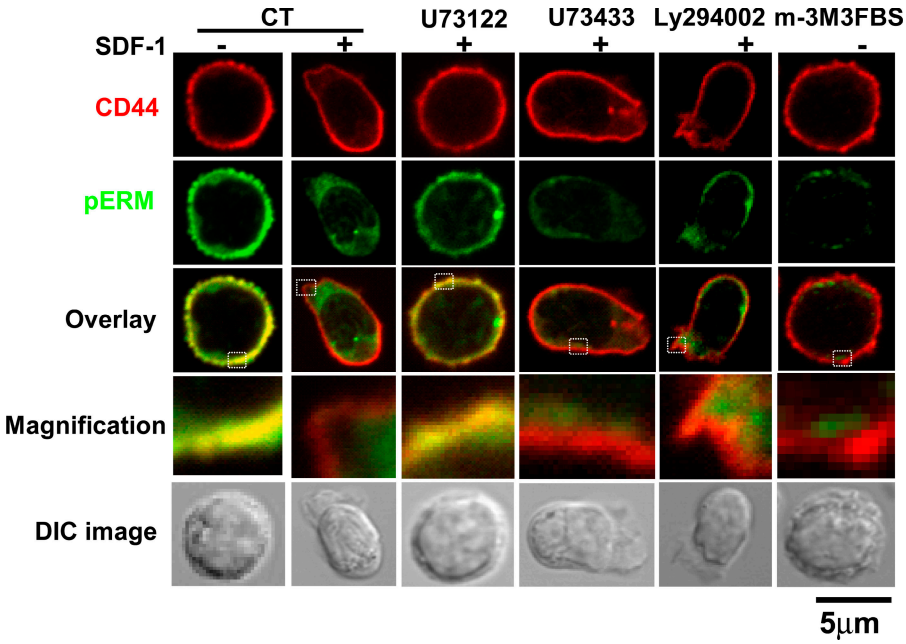

Figure 2. **SDF-1–induced delocalization of ERM proteins from plasma membrane depends on PLC signaling.** Immunofluorescence analysis of PBT treated as in Fig. 1. After treatments, the cells were subjected to fixation and immunofluorescence staining. The third row shows an overlay of CD44 and pERM, and the fourth row shows a higher magnification of boxed regions in the third row, which highlight either colocalization of pERM with CD44 or lack thereof. The fifth row shows differential interference contrast (DIC) images displaying cell polarization. CT, control.

protein inactivation was therefore assessed using two readouts: dephosphorylation of ERM proteins and their dissociation from the membrane. SDF-1–induced ERM protein dephosphorylation is efficiently blocked in peripheral blood T cells (PBTs) pretreated with U73122 but not with U73433, the inactive analogue (Fig. 1 A). Conversely, the PLC activator m-3M3FBS induces ERM protein dephosphorylation. In contrast, the PI3-K inhibitor Ly294002 does not inhibit ERM protein dephosphorylation (Fig. 1 A). Similar results were obtained with the Jurkat T cell line (unpublished data). Thus, PLC activation is necessary for SDF-1–induced rapid ERM protein dephosphorylation and is sufficient to initiate ERM protein dephosphorylation.

Lymphocytes express both moesin and ezrin, which are functionally similar in many respects. However, moesin and ezrin have also been reported to have some functional differences; e.g., in regulation of their localization in T cells (Ilani et al., 2007). Using PAGE conditions optimized for resolving ezrin and moesin, we find that both undergo SDF-1–induced dephosphorylation and that dephosphorylation of both is sensitive to the PLC inhibitor U73122 (Fig. 1, B and C).

Immunofluorescence microscopy of lymphocytes under these stimulation conditions indicated that ERM protein dissociation from membrane accompanies the dephosphorylation (Fig. 2). In untreated primary T lymphocytes, pERM proteins (Fig. 2, green) almost completely colocalize with the transmembrane molecule CD44 (Fig. 2, red) at the cell periphery. The staining of pERM is punctate (consistent with enrichment in microvilli) and strong. After the cells are stimulated with SDF-1, the CD44 remains in the membrane but is often polarized toward the uropod, as previously described (del Pozo et al., 1995). pERM staining is weak (reflecting partial dephosphorylation), diffuse, and not well localized with CD44 (Fig. 2, magnification), indicating that pERM was released from its membrane association. The PLC inhibitor U73122 blocks the SDF-1–induced cell polarization, the decrease in pERM staining, and the delocalization of pERM from the membrane (Fig. 2). The inactive analogue U73433 and the PI3-K inhibitor do not block these processes. In addition, the PLC activator m-3M3FBS was tested to determine whether activation of PLC by itself will lead to ERM protein dephosphorylation and disassociation from the membrane. Indeed, treatment of PBTs with m-3M3FBS induced ERM protein dephosphorylation and disassociation from CD44 (Fig. 2). Thus, PLC mediates SDF-1 stimulation-induced ERM protein dephosphorylation and disassociation from cortical membrane.

A complementary biochemical approach was used to confirm SDF-1–triggered release of ERM proteins from membrane: sonication and ultracentrifugation to separate a membrane-enriched pellet P100 and a soluble (cytosolic) fraction S100 (e.g., Frantz et al., 2007). The results (Fig. 3) show that (a) SDF-1 treatment induces substantial release of moesin and ezrin from the P100 membrane-associated pellet, and (b) the active PLC inhibitor U73122 abrogates that release.

Active PLC induces ERM protein dephosphorylation, release from the membrane, and reduction of membrane PIP2

To verify genetically that the activation of PLC induces ERM protein dephosphorylation, dominant active or inactive PLC constructs were transfected into Jurkat T cells. Transient overexpression of the constitutively active PLC-γ1 NN (having two instances of the N-terminal SH2 domain) construct in Jurkat cells induces ERM protein dephosphorylation (assessed by Western blot [WB]), but the inactive Y783F mutant (Serrano et al., 2005) does not (Fig. 4 A). Immunofluorescent analysis of cells transfected with constitutively active PLC confirms a reduction in pERM and redistribution of the remaining pERM away from the plasma membrane (Fig. 4 B). A complementary approach by which to assess membrane localization of moesin is by cotransfection of the PLC constructs with moesin-GFP (Fig. 4, C [C1/C2] and D). Moesin-GFP is enriched almost twofold at the plasma membrane in the presence of the inactive

Published February 9, 2009

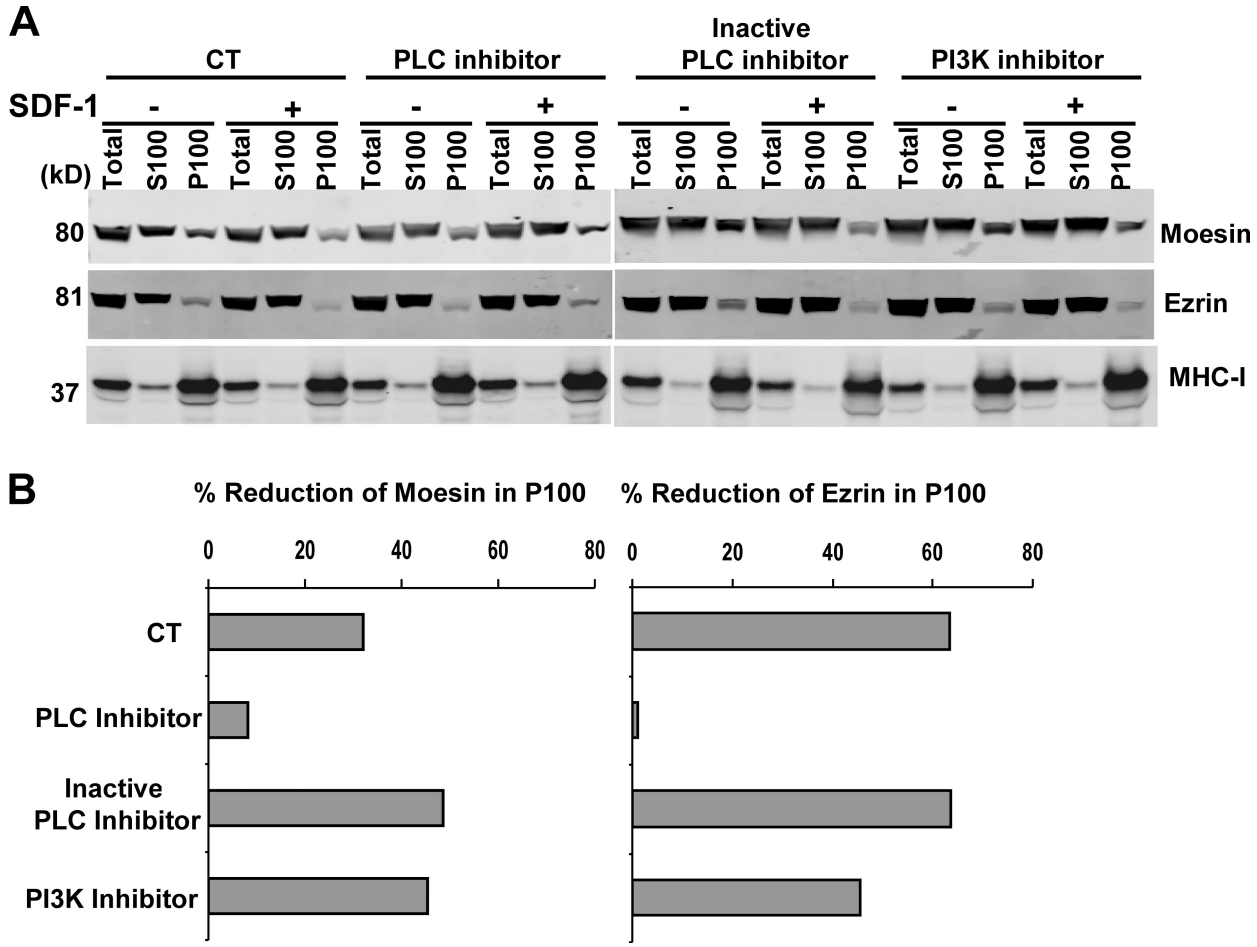

Figure 3. **SDF-1–induced ERM protein release from the membrane-enriched fraction depends on PLC signaling.** (A) Freshly isolated PBTs were pretreated with the indicated inhibitors at 37°C for 15 min, and cells were stimulated with SDF-1 at 37°C for 45 s. Subcellular fractionation by sonication and centrifugation was performed as described in Materials and methods. Total indicates postnuclear supernatant, S100 indicates soluble cytosolic fraction (S100) thereof obtained by centrifugation of postnuclear supernatant at 100,000 *g*, and P100 indicates pellet (P100) whose enrichment in membrane is documented by WB for MHC-I. White line indicates that intervening lanes have been spliced out. (B) Quantitative analysis of data from A by Odyssey software (version 3.0). SDF-1 stimulation induces release of both moesin and ezrin from membrane. This release can only be prevented by PLC inhibitor U73122 but not by PI3-K inhibitor. CT, control.

PLC construct but loses its membrane enrichment in the presence of the constitutively active PLC construct.

The foregoing analyses demonstrate that PLC is necessary and sufficient for ERM protein inactivation but do not address which aspect of PLC signaling is involved. The most investigated aspects of PLC signaling are the second messengers DAG and IP3 (with its attendant Ca^{2+} flux). However, PLC activation also reduces the PIP2 level that, we hypothesized, could mediate ERM protein inactivation. The GFP-tagged pleckstrin homology (PH) domain of PLC-δ (GFP-PH) was used as a reporter for PIP2 levels. In untransfected Jurkat cells, pERM is highly colocalized with the GFP-PH domain, indicating high PIP2 levels in the vicinity of pERM (Fig. 4 B). Transfection of the constitutively active PLC construct abolishes the plasma membrane enrichment of the GFP-PH domain, documenting that it causes reduction in PIP2 (concurrent with inducing dephosphorylation of ERM proteins and delocalization of ERM proteins from the membrane). Moreover, exposure of the cells to either SDF-1 or PLC activator induces redistribution of GFP-PH into the cytoplasm (Fig. 4 E). Thus, these stimulations indeed induce hydrolysis of PIP2.

Reduction of PIP2 concentration induces moesin and ezrin release from cortical membrane in Jurkat cells

To directly test whether the depletion of PIP2 suffices to induce ERM protein dissociation from membrane in cells, we experimentally decreased the levels of PIP2 using a recently described approach involving drug-inducible recruitment of type IV phosphoinositide 5-phosphatase (5-ptase) to the plasma membrane to acutely reduce PIP2 (Heo et al., 2006; Suh et al., 2006; Varnai et al., 2006; van Zeijl et al., 2007). This approach exploits rapamycin-induced heterodimerization of the CFP-tagged plasma membrane–targeted FRB (FK-506–binding protein [FKBP]–rapamycin binding) fragment of mTOR with the monomeric RFP (mRFP)–tagged 5-ptase fused to FKBP12. Upon the addition of rapamycin, the 5-ptase enzyme is recruited to the plasma membrane and causes rapid hydrolysis of PIP2 at the 5 position to generate PI4P. Functionality of this strategy was confirmed by the finding that addition of rapamycin induces the membrane recruitment of 5-ptase and the loss of GFP-PH membrane localization (Fig. 5 A, bottom left; and Fig. S1, available at

Published February 9, 2009

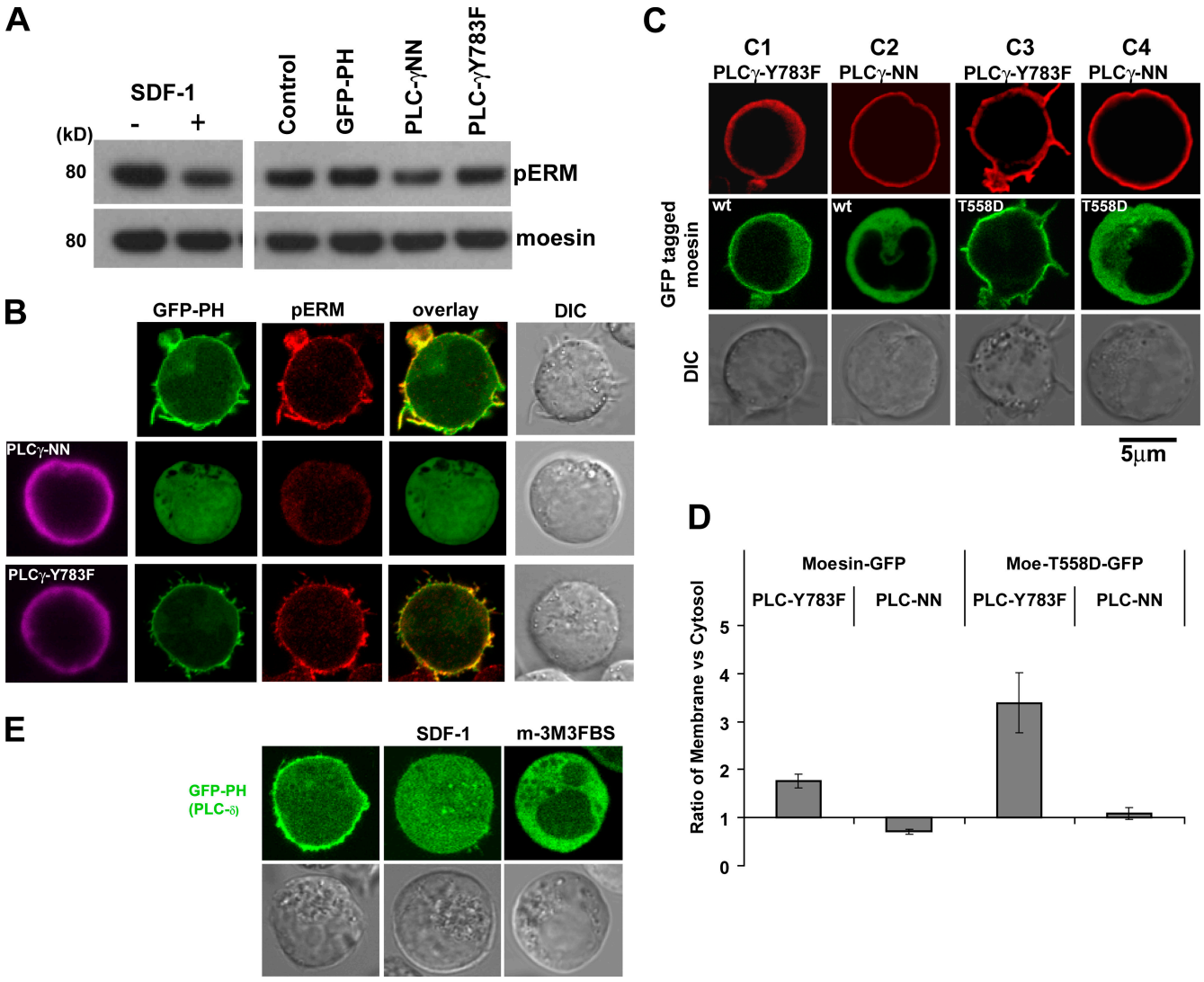

Figure 4. **Transfection with constitutively active PLC induces ERM protein dephosphorylation and release from the plasma membrane.** (A) Jurkat cells were transfected with the indicated PLC-γ1 constructs (NN, constitutively active; or Y783F, inactive) or construct-encoding GFP-PH and analyzed by WB. Expression of PLC-γ1 in Jurkat does not influence the expression of moesin constructs (Fig. S3, available at http://www.jcb.org/cgi/content/full/jcb.200807047/DC1). (B) Imaging of control cells (top) compared with cells transfected with constitutively active NN PLC-γ1 construct (middle) or with inactive PLC-γ1 Y783F (bottom). Markers examined are the transfected PLC (anti-HA antibody, purple), pERM level (red), and transfected GFP-PH localization. (C) Fluorescent analysis of Jurkat cells cotransfected with GFP-moesin (wt or T558D) and PLC-γ1 constructs (detected with anti-HA antibody [red]). (D) Quantitative analysis of data from C (n = 10 for each condition). Quantitative analysis was performed as described in Materials and methods. (E) SDF-1 stimulation induces hydrolysis of PIP2. Jurkat cells were transfected with GFP-tagged PH domain construct and analyzed by immunofluorescence microscopy after SDF-1 or PLC activator treatment. Note that unlike PBTs, Jurkat cells do not undergo striking shape change (polarization) in response to SDF-1. Error bars indicate SEM. DIC, differential interference contrast.

http://www.jcb.org/cgi/content/full/jcb.200807047/DC1). To test whether this inducible reduction of PIP2 can induce dissociation of ERM proteins from the membrane, Jurkat cells were transfected with GFP-tagged moesin and ezrin constructs along with the membrane-targeted FRB-CFP and the mRFP-FKBP–5-ptase domain constructs. Rapamycin-induced recruitment of the 5-ptase to the membrane causes translocation of moesin-GFP and ezrin-GFP into the cytosol (Fig. 5 A and Fig. S1). Quantitative analysis (Fig. 5 B) demonstrates a 1.7-fold enrichment of moesin and a more modest 1.2-fold enrichment of ezrin at the membrane before rapamycin but abolition of that enrichment after rapamycin. Control transfections (in which the 5-ptase construct is replaced by one lacking the ptase domain) show that neither the PH domain reporter nor moesin-GFP loses their membrane enrichment after rapamycin treatment (Fig. 5 A). Thus, PIP2 hydrolysis alone induces release of moesin and ezrin from the plasma membrane.

Moesin and ezrin membrane association is substantially PIP2 dependent even with C-terminal phosphorylation (with or without multilysine mutation)

The relationships between PIP2 binding, C-terminal phosphorylation, membrane association, and conformational activation are central issues in understanding ERM proteins. Therefore, we first assessed whether C-terminal phosphorylation controls

Published February 9, 2009

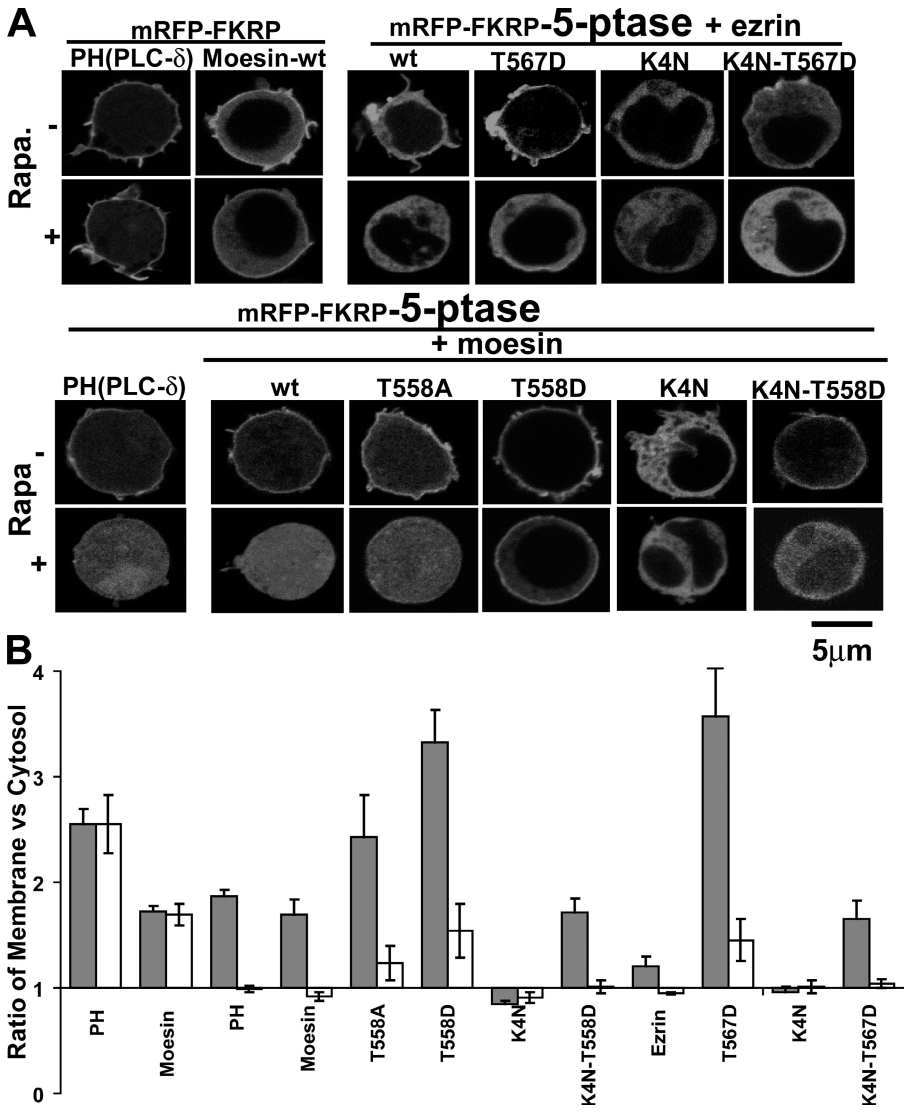

Figure 5. **Membrane translocation of type IV 5-ptase reduces plasma membrane PIP2 and releases moesin and ezrin from the membrane.** (A) Jurkat cells were transfected with GFP-tagged PH domain or the indicated GFP-moesin or GFP-ezrin constructs, along with the membrane-targeted FRB-CFP and the mRFP-FKBP domain constructs (with or without type IV 5-ptase domain as indicated), and were analyzed by fluorescence microscopy before and after rapamycin (Rapa) treatment. GFP fluorescence is shown. mRFP-FKBP, mRFP-FKBP–5-ptase, and FRB-CFP fluorescence images are shown in Fig. S1 (available at http://www.jcb.org/cgi/content/full/jcb.200807047/DC1). (B) Quantitative analysis of the membrane enrichment of moesin, ezrin, or PH domain constructs (n = 10 for each condition) was performed as described in Materials and methods. Error bars indicate SEM.

membrane association by monitoring GFP-tagged phosphomimetic moesin (T558D) in Jurkat cells. The phosphomimetic moesin (T558D) construct was more highly enriched at the plasma membrane than wild type (wt; Fig. 4 D, 3.4 vs. 1.8; and Fig. 5 B, 3.3 vs. 1.7). Surprisingly, the membrane association of the T558D construct was completely disrupted in cells expressing the constitutively active PLC-γ1 NN construct (Fig. 4, C and D). Thus, although ERM protein phosphorylation augments membrane association, action of PLC can abolish membrane association even of the phosphorylated form.

We tested the ability of PIP2 hydrolysis by itself (by 5-ptase recruitment) to trigger disassociation of phosphomimetic moesin (Fig. 5, A and B). After rapamycin treatment, there is marked redistribution of T558D to the cytosol. But even after treatment, the T558D protein has limited residual enrichment at the membrane (unlike wt after rapamycin). The residual enrichment suggests that phosphorylation cooperates (or synergizes) with PIP2 in activating ERM proteins rather than substituting for it (see Discussion). It is interesting that the T558A mutation has a behavior intermediate between wt and T558D (Fig. 5, A and B). We interpret this to indicate that the threonine 558 side chain participates in stabilizing the closure of moesin FERM to C terminus and that mutation of threonine to alanine therefore causes limited relaxation of autoinhibition. Investigation of ezrin confirmed that it resembled moesin in three key respects (Fig. 5, A and B): membrane localization of the wt protein depended on PIP2, the phosphomimetic mutant protein had augmented membrane localization, and the phosphomimetic mutant protein continued to depend on PIP2 for most of its membrane localization.

Exploration of issues related to PIP2-mediated activation of ERMs has been facilitated by the description of an ezrin construct that is defective in PIP2 binding as a result of four K to N mutations (K4N) in the FERM domain (Barret et al., 2000; Fievet et al., 2004). Previous findings that the full-length ezrin K4N mutant fails to associate with the membrane (Barret et al., 2000; Fievet et al., 2004) are confirmed by our investigations of both moesin and ezrin (Fig. 5, A and B). Moreover, our findings confirm those of Fievet et al. (2004) that the mutations mimicking phosphorylation (moesin T558D and ezrin T567D) partially restore membrane association (Fig. 5, A and B). Fievet et al. (2004) interpreted their results to indicate that this association

Published February 9, 2009

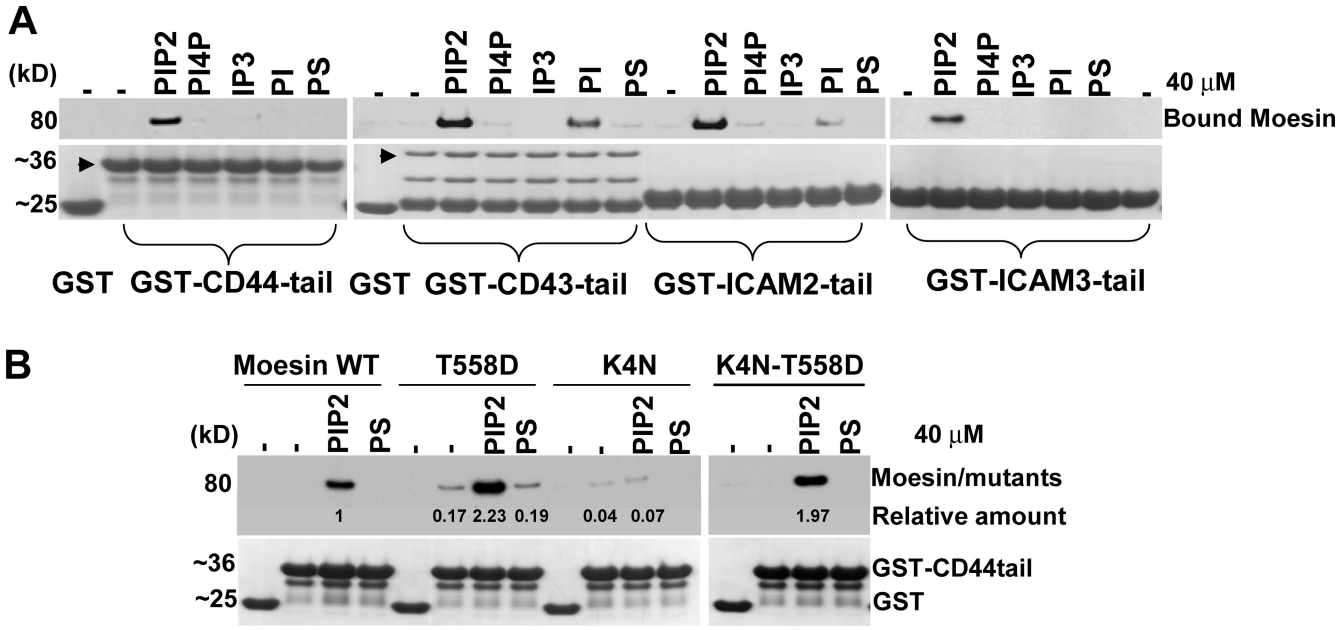

Figure 6. **PIP2 binding is required for the association of moesin with the cytoplasmic tails of CD44, CD43, ICAM2, and ICAM3.** (A) Effects of phospholipids or IP3 on the interaction between moesin and cytoplasmic tails of CD44, CD43, ICAM2, and ICAM3. The bound proteins by GST-tagged tails in the pellet were detected with antimoesin antibody and are shown in the top panel. Arrowheads indicate the intact protein in the lanes where degredation products also exist. (B) The effects of T558D mutation mimicking phosphorylation, K4N mutations, or their combination on the activation of moesin for CD44 tail binding. The bound proteins shown in the top panel were detected by WB. Further characterization of the recombinant protein is shown in Fig. S2 (available at http://www.jcb.org/cgi/content/full/jcb.200807047/DC1). GST (as control) or GST fusion proteins in the pellet were detected with Coomassie blue staining and are shown in the bottom panels. Each lane represents 40% of the amount of protein in the pellet. PI, phosphatidylinositol; PS, phosphatidylserine.

was PIP2 independent. In contrast, our analysis with rapamycin-induced PIP2 hydrolysis indicates that the membrane association of this K4N mutant is still entirely PIP2 dependent (see Discussion). Thus, additional elements of moesin beyond these four K residues can mediate PIP2 binding in intact cells.

PIP2 contributes to opening autoinhibited ERM proteins for binding to CD44, CD43, and ICAMs even with phosphomimetic ERM proteins

ERM proteins have been shown to bind in vitro to cytoplasmic tails of various transmembrane proteins (including CD43, CD44, and ICAMs). Although many of the studies have demonstrated PIP2 dependence of those interactions (Hirao et al., 1996; Heiska et al., 1998; Serrador et al., 2002), some have not demonstrated PIP2 dependence (Yonemura et al., 1998), and often other phospholipids have not been assessed for their ability to replace that requirement. Therefore, we reassessed under standardized conditions whether interaction of the cytoplasmic tails of four transmembrane proteins with moesin depended on phospholipid. The results demonstrate that the binding of all of four GST-tagged tails to moesin is dependent on the presence of PIP2 and is not replaced by phosphatidylserine (Fig. 6 A). It is notable that for each of the four tails, the only other phosphoinositide of reasonable abundance in cellular membrane, PI4P (Stephens et al., 1993; Balla, 2005), is much less efficient in stabilizing the interaction.

Localization of ERM proteins at the cell membrane may be substantially mediated by binding of ERM protein to cytoplasmic tails. If so, in vitro binding of mutant ERM proteins to cytoplasmic tails should depend on PIP2 in a manner similar to that observed with moesin mutant constructs in intact cells. We restricted our analysis of that question to one tail, CD44, because the lipid dependence of the four tails tested is similar. Results of such testing (Fig. 6 B) demonstrate a virtually perfect concordance. The T558D mutant displays enhanced binding in the presence of PIP2 (relative to wt) and a small amount of PIP2-independent binding (not observed in wt) exactly as shown in Fig. 5 A. The K4N shows minimal binding even in the presence of PIP2, but superimposition of the T558D mutation enables PIP2-dependent binding (Fig. 6 B). These findings are the first to demonstrate in vitro that PIP2 binding is required even with a phosphomimetic moesin protein.

Decrease in PIP2 induces dephosphorylation of ERM proteins

The foregoing analyses demonstrate the dominant role of PIP2 rather than phosphorylation in controlling both localization at the cell membrane in cells and binding to cytoplasmic tails in vitro. Therefore, ERM protein dephosphorylation observed during chemokine activation cannot be the prime mediator of ERM protein delocalization from the membrane. Instead, we predicted ERM protein dephosphorylation would result from PIP2 hydrolysis. The model system of rapamycin-induced 5-ptase recruitment allows testing whether PIP2 hydrolysis by itself is sufficient. The results demonstrate that rapamycin treatment induces ERM protein dephosphorylation (Fig. 7, A and B). Thus, hydrolysis of PIP2 triggers ERM protein release from membrane and dephosphorylation.

Published February 9, 2009

Discussion

Rapid inactivation of ERM proteins is especially relevant to hematopoietic cells because of the involvement of ERM proteins in the rapid transition from quiescent spherical cells to polarized migratory cells (Brown et al., 2001). This study addresses three aspects of ERM protein inactivation. First, PLC activity is required for chemokine-mediated dissociation of ERM proteins from the membrane. Second, in contrast to the typical emphasis on DAG and IP3 signaling in hematopoietic cells, our results demonstrate the importance of PIP2 hydrolysis because reduction in PIP2 levels is sufficient to induce ERM protein dissociation from the membrane. Third, our results indicate that ERM phosphorylation is not sufficient to maintain ERM proteins at the membrane. Phosphorylation of ERM proteins also fails to eliminate their dependence on PIP2 for in vitro binding to cytoplasmic tails. Furthermore, reduction in PIP2 in vivo is sufficient to induce ERM protein dephosphorylation. The discussion focuses on integrating these findings into a broader understanding of ERM proteins.

Our study demonstrates that PLC mediates chemokine-induced inactivation of ERM proteins in lymphocytes, which is the first implication of PLC in ERM protein inactivation in any cell type. This inactivation is initiated by chemokine binding to a GPCR, CXCR4, and thus fits the paradigm that PLC activation commonly results from GPCR signaling (Rhee, 2001). Identification of the relevant PLC genes has been impeded by the existence of more than a dozen PLC isoforms. Previous studies implicate PLC β2/β3 as limited contributors to T lymphocyte migration in double knockout mice (Bach et al., 2007), but our experiments do not show a major decrease in chemokine-induced ERM protein dephosphorylation in such mice (unpublished data). We chose PLC-γ1 for our genetic confirmation of PLC's capacity to mediate ERM protein inactivation (Fig. 4) because that isoform is strongly expressed in T cells, and recent evidence indicates that isoform (Dar and Knechtle, 2007) or a closely related isoform (de Gorter et al., 2007) is involved in chemokine-induced migration. Moreover, the T cell receptor also mediates ERM protein dephosphorylation and membrane relaxation (Faure et al., 2004) via a signaling pathway that depends on the same two molecules that mediate PLC-γ1 activation, Vav-1 and Rac1 (Zugaza et al., 2004). Identification of the PLC isoforms that mediate chemokine-induced ERM inactivation in primary T cells is an important question for future research.

This study shows that inactivation of ERMs in lymphocytes by PLC can be explained by PLC-mediated reduction of plasma membrane PIP2. The efficacy of these molecular mechanisms is established using the recently devised strategy for inducing rapid hydrolysis of PIP2 by drug-induced translocation of 5-ptase (Heo et al., 2006; Varnai et al., 2006). This approach provides confirmation of the view that plasma membrane PIP2 is a regulator of processes/assemblies at the plasma membrane, especially cytoskeleton (Janmey and Lindberg, 2004; McLaughlin and Murray, 2005). For example, this approach has been used (a) to characterize regulatory effects of PIP2 on ion channels and gap junctions (Varnai et al., 2006; van Zeijl et al., 2007) and (b) to analyze the role of positively charged clusters of amino acids in recruiting proteins to the plasma membrane via PIP2 (Heo et al., 2006). Finally, and most relevant to this study, EGF-mediated activation of PLC reduces membrane PIP2 and releases cofilin from the plasma membrane (van Rheenen et al., 2007). Both this study and the aforementioned cofilin study corroborate the view that membrane PIP2 is a key regulator of molecules (such as cofilin and ERM proteins) that bind and influence the cortical cytoskeleton.

Although extensive work has been done on ERM protein interaction with phospholipid in vitro, in vivo studies have been limited (Barret et al., 2000; Yonemura et al., 2002; Fievet et al., 2004; Rasmussen et al., 2008). The first in vivo evidence for the hypothesis that PIP2 plays a role in membrane localization of ERM proteins was based on mutational analysis (Barret et al., 2000); the authors mutated pairs of positively charged lysine residues in the FERM domain that they predicted would mediate PIP2 binding and demonstrated that the mutation of two such pairs (a construct we refer to as K4N-moesin) impaired PIP2 binding in vitro and membrane localization in vivo of ERM protein. Yonemura et al. (2002) extended the in vivo understanding greatly by three key findings: ERM protein phosphorylation was not always required for membrane association, enhancing PIP2 by overexpression of PI4P5K-augmented ERM protein membrane association, and microinjection of neomycin reduced ERM membrane association apparently by reduction of available PIP2. The third study implicating PIP2 in ERM protein activation in cells described the use of a membrane-localized lipid phosphatase domain to blunt osmotic stress-induced ERM protein activation (Rasmussen et al., 2008). The fourth key study used the K4N-moesin to explore the relationship between PIP2 binding and phosphorylation and generated results supporting a model that PIP2 binding occurs first, causing release of autoinhibition and consequently enabling phosphorylation (Fievet et al., 2004).

In contrast to the Fievet et al. (2004) study, we show that ERM proteins depend on PIP2 for membrane association even after phosphorylation (Fig. 4, C4; and Fig. 5). Fievet et al. (2004) concluded that PIP2 binding was a mechanism to activate ERM proteins, which after subsequent ERM phosphorylation became unnecessary for membrane binding. Two key elements of our study are critical to the altered interpretation. The first element is the use of drug-induced 5-ptase membrane localization to acutely alter PIP2 levels. This approach allows a clear demonstration that the localization of phosphomimetic moesin protein at the membrane is still dependent on PIP2. The second element is quantitation of the extent of enrichment of wt and mutant moesin constructs at the membrane. Although the phosphomimetic K4N protein is somewhat enriched at the membrane, its degree of enrichment is much less than the corresponding construct without the K4N mutation. Thus, even in the presence of pseudophosphorylation, PIP2 binding by those four K residues is still of major importance.

The foregoing finding, i.e., continued dependence of pERM on PIP2 for membrane association, has critical implications for the process that we set out to study, namely acute inactivation of lymphocyte ERM proteins by chemokine stimulation. If the Fievet model were correct, ERM inactivation should not be inducible by reduction of PIP2 because lymphocyte ERM proteins are substantially phosphorylated in the cortex (Brown et al., 2003), and phosphorylation was interpreted to make ERM

Published February 9, 2009

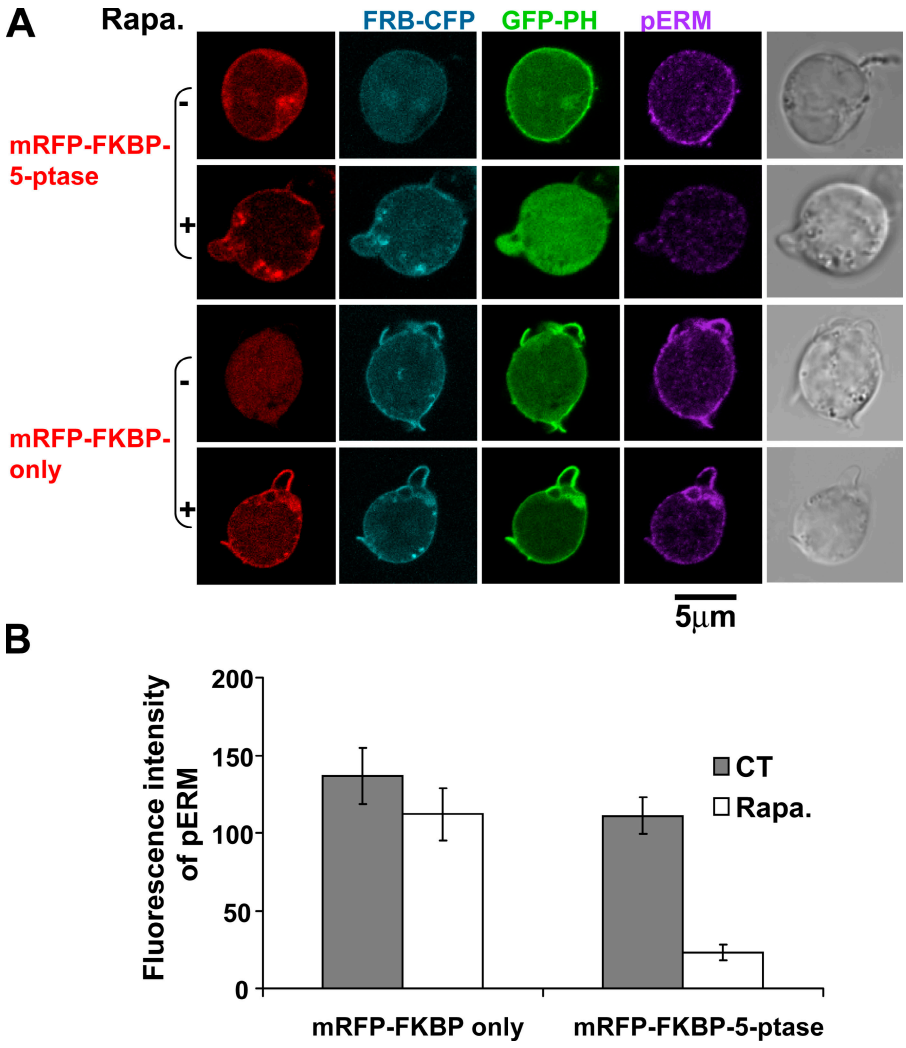

Figure 7. **Type IV 5-ptase mediates decrease of PIP2 and induces endogenous ERM protein dephosphorylation in Jurkat cells.** (A) Immunofluorescence analysis of ERM protein phosphorylation in cells transfected with PH-GFP construct, the membrane-targeted FRB-CFP, and the mRFP-FKBP domain construct (with or without type IV 5-ptase domain as indicated). (B) Quantitative analysis of pERM (n = 10 for each condition). Error bars indicate SEM. Rapa, rapamycin; CT, control.

proteins independent of PIP2 (Fievet et al., 2004). In contrast, because our study shows that pERM continues to depend on PIP2 for membrane association, reduction of PIP2 by PLC is an appealing mechanism for initiating ERM protein inactivation. Indeed, our study demonstrates that PLC activation is necessary for chemokine-induced ERM protein release from the cortex.

Results of in vitro experiments of moesin binding to cytoplasmic tails (Fig. 6) provide a candidate mechanism for the in vivo behavior. They suggest that binding of ERM proteins to cytoplasmic tails directly contributes to the in vivo requirement for PIP2 in ERM protein association with membrane. We extend what was previously known (Fig. 6; Hirao et al., 1996; Heiska et al., 1998; Yonemura et al., 1998; Serrador et al., 2002). First, to address conflicting data in the literature, we directly compared the tails of four relevant cytoplasmic proteins and examined the ability of other phospholipids to replace PIP2 requirement. The results demonstrate that all of the tails are dependent on PIP2 (unlike a previous study [Yonemura et al., 1998]) and that PIP2 cannot be replaced by phosphatidylserine. Second, they demonstrate that phosphorylation cannot replace PIP2 in promoting ERM protein binding to cytoplasmic tails in vitro. Thus, there is a parallel between the failure of phosphorylation to substitute for PIP2 in vitro for binding to cytoplasmic tails and its failure to substitute for PIP2 for enrichment at the membrane in vivo. Therefore, our findings suggest that PLC-mediated inactivation of ERM proteins is dependent in part on reducing the PIP2-dependent binding of ERM to cytoplasmic tails. The mechanism for this PIP2 dependence seems to relate primarily to PIP2-mediated conformation activation of intact ERM proteins rather than to a direct affect on the cytoplasmic tails because binding of cytoplasmic tails to FERM domain (as opposed to intact ERM protein) is not dependent on PIP2 (Hirao et al., 1996; and unpublished data).

It is worth emphasizing that our findings are consistent with preexisting views that (a) PIP2 induces conformational activation that allows C-terminal phosphorylation and that (b) C-terminal phosphorylation also promotes activation (e.g., the finding that moesin T558D shows greater membrane enrichment than wt; Fig. 4 C, C3 vs. C1; and Fig. 5 A, wt vs. T558D). However, our findings contradict the view that C-terminal phosphorylation fully replaces the PIP2 requirement, as seemed to be the conclusions of Fievet et al. (2004). Rather, our evidence supports a more complex view of cooperativity, either for in vivo membrane localization or in vitro association with cytoplasmic tails. Two findings are worth emphasizing in this context. First, in cells, the phosphomimetic moesin construct resembles the wt in depending on PIP2 but unlike the wt cannot be fully dissociated by 5-ptase (Fig. 5 A).

Published February 9, 2009

Second, the most dramatic illustration of this cooperativity is with moesin K4N binding to the CD44 tail. PIP2 alone or the T558D mutation alone has little effect, but the combination dramatically augments binding (Fig. 6 B). It is worth noting that the PIP2 affect in this context must be independent of the K253/254 and K262/263, which have been mutated. Thus, this must reflect an independent structural role of PIP2 in inducing conformational change. The simplest hypothesis is that it reflects the PIP2 binding identified by x-ray crystallography, which promotes conformational change in the FERM domain (Hamada et al., 2000).

Among the rich literature on ERM protein activation, there is considerable work on cellular and biochemical processes that activate ERM. In contrast, this study focuses on the processes that regulate acute inactivation. The results demonstrate for the first time that PLC reduction of membrane PIP2 initiates that inactivation. PIP2 hydrolysis by itself is sufficient to induce ERM protein dephosphorylation, indicating that PIP2 regulation is the primary mediator of both activation and inactivation.

Materials and methods

Cell lines and reagents

Jurkat T cell lines (American Type Culture Collection) were maintained in RPMI 1640 supplemented with 10% fetal bovine serum, 50 µM 2-mercaptoethanol, and penicillin-streptomycin (Invitrogen). Fresh human PBTs were isolated from the blood of healthy human volunteers by leukapheresis and immunomagnetic negative selection as previously described (Brown et al., 2003). The following antibodies were used: pERM mAb pT567, whose reactivity includes moesin pT558, ezrin pT567, and radixin pT564 (BD), rabbit polyclonal antibodies raised against human moesin 473–486, β-actin mouse mAb (Sigma-Aldrich), moesin-specific mAb 38/87 (NeoMarkers), major histocompatibility complex I–specific rabbit mAb (Epitomics), Alexa Fluor 488–conjugated CD44 mAb (BioLegend), and HRP-conjugated Penta-His antibody (QIAGEN). PLC inhibitor U73122, analogue U73433, PI3-K inhibitor Ly294002, and PLC activator m-3M3FBS were purchased from EMD.

DNA constructs and preparation of purified proteins

The PLC-δ1–PH-GFP construct was provided by M. Lemmon (University of Pennsylvania, Philadelphia, PA). CFP-tagged membrane-targeting construct containing FRB domain of human mTOR1 and mRFP-tagged human type IV 5-ptase enzyme construct containing FKBP12 or mRFP-FKBP12 control construct without type IV 5-ptase were provided by T. Balla (National Institute of Child Health and Human Development, Bethesda, MD). The dominant-negative PLC construct Y783F has been previously described (Irvin et al., 2000). The constitutively active PLC-γ1 NN construct was made by replacing the carboxy-terminal SH2 domain with a second copy of the amino-terminal SH2 domain. It was chosen for this study because it is constitutively active in a broader range of cell types than others described previously (DeBell et al., 2007). GFP-tagged constructs of moesin, ezrin, or mutants thereof were prepared in the pEGFP-N1/C1 vector (Clontech Laboratories, Inc.). Full-length moesin, moesin T558D, moesin K4N, and moesin K4N-T558D with His_6 tagged at their C termini were prepared from clones containing their coding DNA in the expression vector pET-23a$^+$ (EMD) or pBAD-Myc-His (Invitrogen). To prepare GST-tagged transmembrane protein cytoplasmic tail constructs, including GST-CD44 (residues 291–361), GST-CD43 (residues 276–400), GST-ICAM2 (residues 247–275), and GST-ICAM3 (residues 508–547), DNA fragments were produced by RT-PCR with primers encoding the corresponding region, using total mRNA isolated from human PBTs and subcloned into BamHI and SalI sites of pGEX-4T-2 (GE Healthcare). Constructs with mutations were generated using the QuikChange site-directed mutagenesis kit (Agilent Technologies). All constructs and mutations were verified by DNA sequencing. Purification of the His_6-tagged proteins was performed with the His-Bind kit (EMD), and purification of the GST fusion proteins was performed as described in the GST Gene Fusion System Handbook (GE Healthcare). Purity was >95% and confirmed by Coomassie blue staining after SDS-PAGE.

SDF-1 treatment, subcellular fractionation, and WB analysis

Freshly isolated PBTs were cultured in medium A (HBSS containing 0.3% BSA) for 2 h at 37°C for recovery (we found this recovery process is important for getting a better response to SDF-1 stimulation). Such PBTs or Jurkat cells were treated with or without SDF-1 at a final concentration of 200 ng/ml at 37°C for 45 s (or an indicated time). For routine WB analysis, samples were immediately lysed with sample buffer containing 0.2% SDS. Samples were homogenized by sonication and boiled for 3 min. For subcellular fractionation, the samples were mixed with an equal volume of 2× sonication buffer (20 mM Hepes, 300 mm NaCl, 2 mM EDTA, protein inhibitor, and 50 nM calyculin A) and immediately sonicated for 3 min at 4°C. Nuclei and cellular debris were pelleted by centrifugation at 2,000 *g* for 5 min at 4°C, and the resulting postnuclear supernatant was fractionated by centrifugation at 100,000 *g* for 1 h at 4°C to obtain the cytosolic fraction (S100) and the membrane-containing pellet (P100). The P100 pellets were washed once with 1× sonication buffer. The S100 and P100 fractions were denatured by boiling in Laemmli sample buffer. For WB analysis, equal volumes of samples from each treatment were resolved by 4–12% SDS-NuPAGE gels (Invitrogen) or 4–20% Tris-glycine gel, transferred to nitrocellulose membranes, and analyzed by WB with the aforementioned antibodies using an infrared imaging system (Odyssey; LI-COR Biosciences) or ECL (GE Healthcare). In the experiments with inhibitors, the cells were pretreated with the indicated inhibitors (2.5 µM U73122 for PLC or analogue U73433; or 10 µM Ly294002 for PI3-K) at 37°C for 10 min and stimulation with 200 ng/ml SDF-1 for 45 s (or an indicated time). PLC activator m-3M3FBS treatment was done as with SDF-1 stimulation except using 200 µM m-3M3FBS.

Immunofluorescence microscopy

For immunofluorescence analysis of cells with SDF-1 stimulation, PBTs at 10^6 cells in 300 µl of medium A with/without inhibitors, as indicated in Fig. 1, were incubated for 10 min at 37°C and dropped onto the glass bottom of 35-mm cultureware dishes (MatTek) precoated with poly-L-lysine (Sigma-Aldrich). Cells were allowed to settle for 10 min at 37°C, and 1.0 ml of medium A with/without SDF-1 (200 ng/ml final) was added into each dish to stimulate cells for 45 s at 37°C. Cells were fixed by the addition of ice-cold 4% paraformaldehyde solution (Sigma-Aldrich). After 10 min at RT, samples were washed with PBS, permeabilized with 0.2% Triton X-100, and blocked for 1 h at RT in PBS with 3% BSA. Primary antibodies were added for 1 h at RT in PBS with 3% BSA. After washing, Alexa Fluor 546– and/or 488–conjugated secondary antibodies (Invitrogen) in PBS with 3% BSA were added for 1 h at RT. Samples were examined, and images were collected using a confocal microscope (LSM510 META; Carl Zeiss, Inc.) equipped with a Plan Apochromat 63× NA 1.4 oil immersion objective lens (Carl Zeiss, Inc.). The images were organized into figures using Photoshop (version 8.0; Adobe).

For translocation analysis of GFP-tagged constructs in individual cells, Jurkat cells were transfected with the various constructs (5 µg DNA/plasmid) using an electroporator (300 V for 10 ms; BTX ECM 830; Harvard Apparatus). After electroporation, the cells were cultured for 48 h and used for analysis. For analysis of translocation of ERM protein, the cells were collected, washed once with PBS, and resuspended in medium A (prewarmed at 37°C), and the cells at ∼10^6 cells in 200 µl were dropped onto the glass bottom of 35-mm cultureware dishes (MatTek) precoated with poly-L-lysine and were allowed to settle for 10 min at 37°C. 1.0 ml of medium containing 0.36 µM rapamycin was added into the dish. After 5 min of incubation at 37°C, the media was poured off, and the cells were fixed by the addition of ice-cold 4% paraformaldehyde solution immediately. After 10 min at RT, the cells were washed four times with PBS and examined using the same confocal microscopy configuration as for PBT. Quantitative analysis was performed using the Imaging Examiner software (LSM; Carl Zeiss, Inc.). Because fluorescence intensity was not uniform along the plasma membrane, quantitation along a single line across the cell was not sufficiently robust. Instead, for each cell analyzed, a circumferential line was drawn manually at the plasma membrane, and another line was drawn just inside the plasma membrane in the cytosol. Membrane enrichment for that cell is calculated as the mean fluorescence of all pixels on the plasma membrane line divided by the mean fluorescence of all pixels on the cytosol line, and enrichment reported for a cell preparation is the mean for 10 randomly chosen transfected cells.

In vitro pull-down analysis of the interaction with GST-tagged cytoplasmic tails of transmembrane protein

In brief, 1.0 µM purified moesin (wild type or mutants) was incubated with a five times molar excess of glutathione–Sepharose 4B bead-immobilized GST-tagged tail proteins in the presence of the indicated phospholipids (sonicated as described previously [Hirao et al., 1996]; Avanti Polar

Lipids, Inc.) or IP3 (dissolved in water; Avanti Polar Lipids, Inc.) in 150 µl of buffer A (20 mM Tris-HCl, pH 7.5, 1 mM EGTA, 150 mM NaCl, 1 mM DTT, and 0.05% Tween 20) and incubated at 4°C on a rotating wheel for 90 min. After centrifugation (600 *g* for 3 min), the beads were washed twice with buffer A and dissolved in 20 µl of 2× SDS-loading buffer. Two identical sets of samples were run using Nu-PAGE Bis-Tris gels (Invitrogen). One set of samples is used for detecting the amount of moesin or mutants bound in the beads by immunoblotting using antimoesin antibody or Penta-His antibody, and another one is used for visualizing GST-tagged proteins by Coomassie blue staining after separation by SDS-PAGE.

Online supplemental material

Fig. S1 shows that recruitment of type IV 5-ptase to plasma membrane triggers the translocation of PIP2 marker, moesin, or moesin mutant constructs into cytosol. Fig. S2 shows characterization of purified recombinant proteins by Coomassie blue staining after SDS-PAGE. Fig. S3 shows that expression of PLC-γ1 in Jurkat does not influence the expression of moesin constructs. Online supplemental material is available at http://www.jcb.org/cgi/content/full/jcb.200807047/DC1.

We thank Drs. Geoffrey Kansas and Larry Wahl, the National Institutes of Health Clinical Center transfusion service for generous provision of reagents and/or cells, Drs. Tamas Balla and Mark Lemmon for constructs, and Dr. Tamas Balla, Natasha Belkina, Trian Chavakis, and Ling Ren for insightful discussions.

This research was supported by the National Cancer Institute Intramural Research Programs of the National Institutes of Health.

Submitted: 8 July 2008
Accepted: 8 January 2009

References

Bach, T.L., Q.M. Chen, W.T. Kerr, Y. Wang, L. Lian, J.K. Choi, D. Wu, M.G. Kazanietz, G.A. Koretzky, S. Zigmond, and C.S. Abrams. 2007. Phospholipase cbeta is critical for T cell chemotaxis. *J. Immunol.* 179:2223–2227.

Bacon, K.B., L. Flores-Romo, P.F. Life, D.D. Taub, B.A. Premack, S.J. Arkinstall, T.N. Wells, T.J. Schall, and C.A. Power. 1995. IL-8-induced signal transduction in T lymphocytes involves receptor-mediated activation of phospholipases C and D. *J. Immunol.* 154:3654–3666.

Balla, T. 2005. Inositol-lipid binding motifs: signal integrators through protein-lipid and protein-protein interactions. *J. Cell Sci.* 118:2093–2104.

Barret, C., C. Roy, P. Montcourrier, P. Mangeat, and V. Niggli. 2000. Mutagenesis of the phosphatidylinositol 4,5-bisphosphate (PIP_2) binding site in the NH_2-terminal domain of ezrin correlates with its altered cellular distribution. *J. Cell Biol.* 151:1067–1080.

Bretscher, A., K. Edwards, and R.G. Fehon. 2002. ERM proteins and merlin: integrators at the cell cortex. *Nat. Rev. Mol. Cell Biol.* 3:586–599.

Brown, M.J., J.A. Hallam, E. Colucci-Guyon, and S. Shaw. 2001. Rigidity of circulating lymphocytes is primarily conferred by vimentin intermediate filaments. *J. Immunol.* 166:6640–6646.

Brown, M.J., R. Nijhara, J.A. Hallam, M. Gignac, K.M. Yamada, S.L. Erlandsen, J. Delon, M. Kruhlak, and S. Shaw. 2003. Chemokine stimulation of human peripheral blood T lymphocytes induces rapid dephosphorylation of ERM proteins, which facilitates loss of microvilli and polarization. *Blood.* 102:3890–3899.

Cronshaw, D.G., A. Kouroumalis, R. Parry, A. Webb, Z. Brown, and S.G. Ward. 2006. Evidence that phospholipase-C-dependent, calcium-independent mechanisms are required for directional migration of T-lymphocytes in response to the CCR4 ligands CCL17 and CCL22. *J. Leukoc. Biol.* 79:1369–1380.

Dar, W.A., and S.J. Knechtle. 2007. CXCR3-mediated T-cell chemotaxis involves ZAP-70 and is regulated by signalling through the T-cell receptor. *Immunology.* 120:467–485.

de Gorter, D.J., E.A. Beuling, R. Kersseboom, S. Middendorp, J.M. van Gils, R.W. Hendriks, S.T. Pals, and M. Spaargaren. 2007. Bruton's tyrosine kinase and phospholipase Cgamma2 mediate chemokine-controlled B cell migration and homing. *Immunity.* 26:93–104.

DeBell, K., L. Graham, I. Reischl, C. Serrano, E. Bonvini, and B. Rellahan. 2007. Intramolecular regulation of phospholipase C-gamma1 by its C-terminal Src homology 2 domain. *Mol. Cell. Biol.* 27:854–863.

del Pozo, M.A., P. Sanchez-Mateos, M. Nieto, and F. Sanchez-Madrid. 1995. Chemokines regulate cellular polarization and adhesion receptor redistribution during lymphocyte interaction with endothelium and extracellular matrix. Involvement of cAMP signaling pathway. *J. Cell Biol.* 131:495–508.

Delon, J., K. Kaibuchi, and R.N. Germain. 2001. Exclusion of CD43 from the immunological synapse is mediated by phosphorylation-regulated relocation of the cytoskeletal adaptor moesin. *Immunity.* 15:691–701.

Faure, S., L.I. Salazar-Fontana, M. Semichon, V.L. Tybulewicz, G. Bismuth, A. Trautmann, R.N. Germain, and J. Delon. 2004. ERM proteins regulate cytoskeleton relaxation promoting T cell-APC conjugation. *Nat. Immunol.* 5:272–279.

Fievet, B., D. Louvard, and M. Arpin. 2007. ERM proteins in epithelial cell organization and functions. *Biochim. Biophys. Acta.* 1773:653–660.

Fievet, B.T., A. Gautreau, C. Roy, L. Del Maestro, P. Mangeat, D. Louvard, and M. Arpin. 2004. Phosphoinositide binding and phosphorylation act sequentially in the activation mechanism of ezrin. *J. Cell Biol.* 164:653–659.

Frantz, C., A. Karydis, P. Nalbant, K.M. Hahn, and D.L. Barber. 2007. Positive feedback between Cdc42 activity and H^+ efflux by the Na-H exchanger NHE1 for polarity of migrating cells. *J. Cell Biol.* 179:403–410.

Hamada, K., T. Shimizu, T. Matsui, S. Tsukita, and T. Hakoshima. 2000. Structural basis of the membrane-targeting and unmasking mechanisms of the radixin FERM domain. *EMBO J.* 19:4449–4462.

Heiska, L., K. Alfthan, M. Gronholm, P. Vilja, A. Vaheri, and O. Carpen. 1998. Association of ezrin with intercellular adhesion molecule-1 and -2 (ICAM-1 and ICAM-2). Regulation by phosphatidylinositol 4, 5-bisphosphate. *J. Biol. Chem.* 273:21893–21900.

Heo, W.D., T. Inoue, W.S. Park, M.L. Kim, B.O. Park, T.J. Wandless, and T. Meyer. 2006. PI(3,4,5)P3 and PI(4,5)P2 lipids target proteins with polybasic clusters to the plasma membrane. *Science.* 314:1458–1461.

Hirao, M., N. Sato, T. Kondo, S. Yonemura, M. Monden, T. Sasaki, Y. Takai, S. Tsukita, and S. Tsukita. 1996. Regulation mechanism of ERM (ezrin/radixin/moesin) protein/plasma membrane association: possible involvement of phosphatidylinositol turnover and Rho-dependent signaling pathway. *J. Cell Biol.* 135:37–51.

Huang, L., T.Y. Wong, R.C. Lin, and H. Furthmayr. 1999. Replacement of threonine 558, a critical site of phosphorylation of moesin in vivo, with aspartate activates F-actin binding of moesin. Regulation by conformational change. *J. Biol. Chem.* 274:12803–12810.

Hughes, S.C., and R.G. Fehon. 2007. Understanding ERM proteins–the awesome power of genetics finally brought to bear. *Curr. Opin. Cell Biol.* 19:51–56.

Ilani, T., C. Khanna, M. Zhou, T.D. Veenstra, and A. Bretscher. 2007. Immune synapse formation requires ZAP-70 recruitment by ezrin and CD43 removal by moesin. *J. Cell Biol.* 179:733–746.

Irvin, B.J., B.L. Williams, A.E. Nilson, H.O. Maynor, and R.T. Abraham. 2000. Pleiotropic contributions of phospholipase C-gamma1 (PLC-gamma1) to T-cell antigen receptor-mediated signaling: reconstitution studies of a PLC-gamma1-deficient Jurkat T-cell line. *Mol. Cell. Biol.* 20:9149–9161.

Ivetic, A., and A.J. Ridley. 2004. Ezrin/radixin/moesin proteins and Rho GTPase signalling in leucocytes. *Immunology.* 112:165–176.

Janmey, P.A., and U. Lindberg. 2004. Cytoskeletal regulation: rich in lipids. *Nat. Rev. Mol. Cell Biol.* 5:658–666.

Laudanna, C., and R. Alon. 2006. Right on the spot. Chemokine triggering of integrin-mediated arrest of rolling leukocytes. *Thromb. Haemost.* 95:5–11.

Li, Q., M.R. Nance, R. Kulikauskas, K. Nyberg, R. Fehon, P.A. Karplus, A. Bretscher, and J.J. Tesmer. 2007. Self-masking in an intact ERM-merlin protein: an active role for the central alpha-helical domain. *J. Mol. Biol.* 365:1446–1459.

Matsui, T., M. Maeda, Y. Doi, S. Yonemura, M. Amano, K. Kaibuchi, S. Tsukita, and S. Tsukita. 1998. Rho-kinase phosphorylates COOH-terminal threonines of ezrin/radixin/moesin (ERM) proteins and regulates their head-to-tail association. *J. Cell Biol.* 140:647–657.

McLaughlin, S., and D. Murray. 2005. Plasma membrane phosphoinositide organization by protein electrostatics. *Nature.* 438:605–611.

Nakamura, F., L. Huang, K. Pestonjamasp, E.J. Luna, and H. Furthmayr. 1999. Regulation of F-actin binding to platelet moesin in vitro by both phosphorylation of threonine 558 and polyphosphatidylinositides. *Mol. Biol. Cell.* 10:2669–2685.

Niggli, V., and J. Rossy. 2008. Ezrin/radixin/moesin: versatile controllers of signaling molecules and of the cortical cytoskeleton. *Int. J. Biochem. Cell Biol.* 40:344–349.

Pearson, M.A., D. Reczek, A. Bretscher, and P.A. Karplus. 2000. Structure of the ERM protein moesin reveals the FERM domain fold masked by an extended actin binding tail domain. *Cell.* 101:259–270.

Rasmussen, M., R.T. Alexander, B.V. Darborg, N. Mobjerg, E.K. Hoffmann, A. Kapus, and S.F. Pedersen. 2008. Osmotic cell shrinkage activates ezrin/radixin/moesin (ERM) proteins: activation mechanisms and physiological implications. *Am. J. Physiol. Cell Physiol.* 294:C197–C212.

Rhee, S.G. 2001. Regulation of phosphoinositide-specific phospholipase C. *Annu. Rev. Biochem.* 70:281–312.

Rose, D.M., R. Alon, and M.H. Ginsberg. 2007. Integrin modulation and signaling in leukocyte adhesion and migration. *Immunol. Rev.* 218:126–134.

Serrador, J.M., M. Vicente-Manzanares, J. Calvo, O. Barreiro, M.C. Montoya, R. Schwartz-Albiez, H. Furthmayr, F. Lozano, and F. Sanchez-Madrid. 2002. A novel serine-rich motif in the intercellular adhesion molecule 3 is critical for its ezrin/radixin/moesin-directed subcellular targeting. *J. Biol. Chem.* 277:10400–10409.

Serrano, C.J., L. Graham, K. DeBell, R. Rawat, M.C. Veri, E. Bonvini, B.L. Rellahan, and I.G. Reischl. 2005. A new tyrosine phosphorylation site in PLC gamma 1: the role of tyrosine 775 in immune receptor signaling. *J. Immunol.* 174:6233–6237.

Smit, M.J., P. Verdijk, E.M. van der Raaij-Helmer, M. Navis, P.J. Hensbergen, R. Leurs, and C.P. Tensen. 2003. CXCR3-mediated chemotaxis of human T cells is regulated by a Gi- and phospholipase C-dependent pathway and not via activation of MEK/p44/p42 MAPK nor Akt/PI-3 kinase. *Blood.* 102:1959–1965.

Soriano, S.F., A. Serrano, P. Hernanz-Falcon, A. Martin de Ana, M. Monterrubio, C. Martinez, J.M. Rodriguez-Frade, and M. Mellado. 2003. Chemokines integrate JAK/STAT and G-protein pathways during chemotaxis and calcium flux responses. *Eur. J. Immunol.* 33:1328–1333.

Stephens, L.R., T.R. Jackson, and P.T. Hawkins. 1993. Agonist-stimulated synthesis of phosphatidylinositol(3,4,5)-trisphosphate: a new intracellular signalling system? *Biochim. Biophys. Acta.* 1179:27–75.

Suh, B.C., T. Inoue, T. Meyer, and B. Hille. 2006. Rapid chemically induced changes of PtdIns(4,5)P2 gate KCNQ ion channels. *Science.* 314:1454–1457.

van Rheenen, J., X. Song, W. van Roosmalen, M. Cammer, X. Chen, V. Desmarais, S.C. Yip, J.M. Backer, R.J. Eddy, and J.S. Condeelis. 2007. EGF-induced PIP_2 hydrolysis releases and activates cofilin locally in carcinoma cells. *J. Cell Biol.* 179:1247–1259.

van Zeijl, L., B. Ponsioen, B.N. Giepmans, A. Ariaens, F.R. Postma, P. Varnai, T. Balla, N. Divecha, K. Jalink, and W.H. Moolenaar. 2007. Regulation of connexin43 gap junctional communication by phosphatidylinositol 4,5-bisphosphate. *J. Cell Biol.* 177:881–891.

Varnai, P., B. Thyagarajan, T. Rohacs, and T. Balla. 2006. Rapidly inducible changes in phosphatidylinositol 4,5-bisphosphate levels influence multiple regulatory functions of the lipid in intact living cells. *J. Cell Biol.* 175:377–382.

Yonemura, S., M. Hirao, Y. Doi, N. Takahashi, T. Kondo, S. Tsukita, and S. Tsukita. 1998. Ezrin/radixin/moesin (ERM) proteins bind to a positively charged amino acid cluster in the juxta-membrane cytoplasmic domain of CD44, CD43, and ICAM-2. *J. Cell Biol.* 140:885–895.

Yonemura, S., T. Matsui, S. Tsukita, and S. Tsukita. 2002. Rho-dependent and -independent activation mechanisms of ezrin/radixin/moesin proteins: an essential role for polyphosphoinositides in vivo. *J. Cell Sci.* 115:2569–2580.

Zeidan, Y.H., R.W. Jenkins, and Y.A. Hannun. 2008. Remodeling of cellular cytoskeleton by the acid sphingomyelinase/ceramide pathway. *J. Cell Biol.* 181:335–350.

Zugaza, J.L., M.J. Caloca, and X.R. Bustelo. 2004. Inverted signaling hierarchy between RAS and RAC in T-lymphocytes. *Oncogene.* 23:5823–5833.